another combination of a pair of numerical values for them may produce similar result. Other experimental studies using techniques such as light or neutron scattering will be helpful to fix the indexes directly.

VII. Conclusion and Discussion

We have introduced two indexes to characterize spatial structure of a polymeric aggregate formed in a solution through ionic pairing. A general theory to infer their values from viscosity measurement has been developed on the basis of a multiple-equilibria theory of association. Since the treatment of the viscosity curve in our theory is general enough, it can be applied to another colloidal solutions, including those such as latex in oil or red cells in blood. In the latter system it is well-known that aggregates called *rouleaux* in fact control the blood viscosity through association and dissociation processes. This is an example of a system whose solution viscosity has an absolute meaning in its own right.

Looking at the problem from the rheological point of view, temperature and shear rate dependence of the viscosity can provide extensive clues for understanding the nature of association taking place in ionomer solutions. A series of viscosity–temperature measurements[2] showed that very strong and durable interchain networks were formed and persisted up to 150 °C. It was also proved experimentally[1] that viscosity in Couette flow increased with increasing shear, attained a maximum, and then fell again at higher shear rates. The shear-induced thickening phenomena were understood[5] to be caused by elongation of polymer chains under shear. Elongation might promote reaction between ions on different chains at the expense of associations within a chain. Theoretical studies are required for further quantitative understanding of dynamic properties of associating ionomers.

References and Notes

(1) Lundberg, R. D.; Makowski, H. S. *J. Polym. Sci., Polym. Phys. Ed.* **1980**, *18*, 1821. Lundberg, R. D.; Phillips, R. R. *Ibid.* **1982**, *20*, 1143. Peiffer, D. G.; Lundberg, R. D. *Ibid.* **1984**, *22*, 2051.
(2) Agarwal, P. K.; Makowski, H. S.; Lundberg, R. D. *Macromolecules* **1980**, *13*, 1679. Agarwal, P. K.; Lundberg, R. D. *Ibid.* **1984**, *17*, 1918. Agarwal, P. K.; Lundberg, R. D. *Ibid.* **1984**, *17*, 1928. Agarwal, P. K.; Garner, R. T.; Lundberg, R. D. *Ibid.* **1984**, *17*, 2794.
(3) Kim, M. W.; Peiffer, D. G. *J. Chem. Phys.* **1985**, *83*, 4159. Peiffer, D. G.; Kaladas, J.; Duvdevani, I. *Macromolecules* **1987**, *20*, 1397.
(4) Wolf, C.; Silberberg, A.; Priel, Z.; Layec-Raphalen, M. N. *Polymer* **1979**, *20*, 281.
(5) Witten, T. A., Jr.; Cohen, M. H. *Macromolecules* **1985**, *18*, 1915.
(6) Cates, M. E.; Witten, T. A., Jr. *Macromolecules* **1986**, *19*, 72.
(7) Flory, P. J. *Principles of Polymer Chemistry*; Cornell University Press: Ithaca, NY, 1953; Chapter 14.
(8) Tanaka, F.; Ushiki, H. *J. Chem. Phys.* **1986**, *84*, 5925.
(9) Chapter 12 of ref 7.
(10) *On Growth And Form: Fractal and Non-Fractal Patterns in Physics*; Stanley, H. E., Ostrowsky, N., Eds.; Nijhoff: Hingham, MA, 1986.
(11) Israelachvili, J. N. *Physics of Amphiphiles: Micelles, Vesicles and Microemulsions* Degiorgio, V., Corti, M., Eds.; North-Holland: Amsterdam, 1985; p 24.

Complexation of Stereoregular Poly(methyl methacrylates). 11. A Mechanistic Model for Stereocomplexation in the Bulk

Elwin Schomaker and Ger Challa*

Laboratory of Polymer Chemistry, State University of Groningen, Nijenborgh 16, 9747 AG Groningen, The Netherlands.

Received July 22, 1987; Revised Manuscript Received November 13, 1987

ABSTRACT: The process of stereocomplexation between isotactic and syndiotactic PMMA in the bulk was studied by means of differential scanning calorimetry and wide-angle X-ray scattering as a function of annealing time and temperature. It appeared that in all cases the material obtained was partly crystalline. For low annealing temperatures the samples showed multiple endotherms with different characteristics. A mechanistic model, in which subsequent crystallization of the complexed chain sections plays an important role, is presented which accounts for the observed phenomena. At low annealing temperatures complexation proceeds much faster than subsequent crystallization resulting in a fringed-micellar kind of growth, while at higher annealing temperatures lamellar crystallization occurs directly. The endotherms are interpreted respectively as the decomplexation of complexed sections partly organized into fringed-micellar clusters of complexes (T_m^1) and the simultaneous decomplexation and melting of lamellarly crystallized complexes (T_m^3). Apart from these main endotherms also a small endotherm was found (T_m^2), which was assigned to the decomplexation of complexed sections, formed during scanning. The critical sequence length necessary for complexation and the mobility of the chains, and consequently the annealing temperature and molar mass of the polymers employed, are the most important parameters in the mechanistic scheme presented.

Introduction

Ever since the first report of Fox et al.[1] on mixtures of isotactic (i) and syndiotactic (s) poly(methyl methacrylate) (PMMA) showing crystallinity, various papers have been published on the phenomenon of stereocomplexation between i- and s-PMMA, a concept introduced by Liquori et al.[2] Nevertheless the process is still not completely understood. Vorenkamp et al. proved the complexation stoichiometry to be 1 i-unit:2 s-units at the level of monomeric units.[3] Bosscher et al. found that stereocomplexes were also formed when the methyl group of the ester of s-PMMA was replaced by an ethyl or even a *tert*-butyl group, while a modification of the ester group of i-PMMA prevented the formation of stereocomplexes.[4] On the grounds of these observations, conformational energy calculations, and fiber X-ray diffraction data they suggested for the structure of the stereocomplex a 30/4 i-helix surrounded by a 60/4 s-helix.[5]

Complexation is possible in bulk as well as in (dilute) solution. With respect to dilute solution three kinds of

0024-9297/88/2221-2195$01.50/0

solvents can be distinguished: strongly, weakly, and noncomplexing respectively called solvent types A, B, and C.[6,7] In the case of strongly complexing solvents, compact particles are formed with diameters of about 10–30 nm.[8–12]

A very important parameter in the case of complexation reactions is the critical chain length necessary for complexation, defined as the minimum chain length that is necessary to form a stable complex with respect to thermal fluctuations. This parameter depends on the solvent, temperature, and concentration employed.[11,13–17] In case of samples of high molar mass or samples of low tacticity it is better to talk of a critical sequence length, as in these cases different sections of the same chain can form a complex with other complementary chains. For kinetic reasons, as these systems become completely immobilized, a real thermodynamic equilibrium will not be reached in practice. In particular this applies to complexation in the bulk, a possibility which was first shown to occur by Feitsma et al.[18] In the bulk as well as in solution crystallites of stereocomplexes are formed as appears from X-ray diffraction data.[2,3,5,18–21] In different cases multiple endotherms have been observed.[6,21,22] Various explanations have been given for this behavior, ranging from the melting of s-PMMA crystallites next to crystallites of the stereocomplex,[21] to the melting of primary crystallites next to secondary crystallites of stereocomplex,[3] to disintegration of aggregates of stereocomplex particles next to the melting of the particles.[22] Unfortunately none of these theories have been able to explain all observations and data available. A remarkable fact is that until now, the decomplexation step was never considered to be responsible for one of the endotherms, although the stabilization energy of the helix was calculated to be on the order of magnitude of 30 kJ/base mol of complex, consisting of one i-unit and two s-units.[5] In addition to this it should be mentioned that Feitsma et al. have shown that heating complexed material up to 240 °C, which is just beyond both melting endotherms, resulted in the disappearance of the solvent and/or thermal history of the sample.[18] From this finding it was concluded that at this temperature complete decomplexation is reached.

As part of an investigation on the mechanism of stereocomplexation, previous data on the complexation in bulk, published earlier by our laboratory, were reexamined thoroughly and the process was studied by means of DSC and WAXS as a function of annealing time and temperature, resulting in the presentation of a possible mechanism which is able to explain the observations published with respect to this subject, including the multiple melting endotherms.

Because of the complexity of the subject, a slightly different form of presentation is chosen. After the Experimental Section, some characteristic data and observations are summarized qualitatively, without an extensive discussion. Next a mechanistic model for the overall stereocomplexation process is presented and the data will be discussed in more detail. Finally, additional experimental evidence is presented and discussed.

Experimental Section

Materials. Data on the PMMA samples used are listed in Table I. All i-PMMA's were synthesized in toluene with phenylmagnesium bromide as initiator.[23] **i1** and **i2** were obtained by means of fractionation of the product with acetone as solvent and water as precipitant. **i3** was fractionated by precipitation from acetone in boiling methanol. **s2** and **s3** are fractions of products of Ziegler–Natta polymerizations in toluene with triethylaluminum and titanium tetrachloride as catalysts at −78 °C.[24] s1 was prepared from s-poly(methacrylic acid) by methylation with diazomethane in DMF. The poly(methacrylic acid) sample was obtained directly by ^{60}Co radiation polymerization of the monomer in isopropyl alcohol.[25,26]

Table I
Molar Mass and Stereoregularity of the PMMA Samples Used

polymer	$\bar{M}_w$	$\bar{M}_n$	i:h:s, %
i1	3.2×10^4	2.6×10^4	i, >95
i2	$>1 \times 10^6$	$\simeq 1 \times 10^6$	i, >95
i4	7.0×10^5	5.2×10^5	i, >95
s1	8.5×10^4	3.8×10^4	2:7:91
s2	$>1 \times 10^6$	$\simeq 1 \times 10^6$	1:8:91
s3	6.2×10^5	3.1×10^5	1:8:91

Tacticities based on triads were derived from the α-methyl peaks obtained for 3 wt % solutions in o-dichlorobenzene at 120 °C by means of 200-MHz NMR spectroscopy with a Nicolet NT-200.

The molar masses were determined by means of gel permeation chromatography (Waters ALC/GPC 150 C equipped with 2 TSK GMH 6 columns) using THF as eluent, relative to polystyrene standards, employing the method of universal calibration. The following Mark–Houwink constants were used: polystyrene, $K = 1.64 \times 10^{-4}$ dL/g, $a = 0.702$;[32] it-PMMA $K = 1.66 \times 10^{-4}$ dL/g, $a = 0.66$.[33] For st-PMMA the constants of at-PMMA were taken: $K = 1.28 \times 10^{-4}$ dL/g, $a = 0.69$.[34]

Differential Scanning Calorimetry. The samples were prepared by mixing 1 wt % solutions of i- and s-PMMA in chloroform (a so-called noncomplexing solvent) and subsequent precipitation in petroleum ether (bp 40–60 °C). Before annealing in a calibrated oven, the blends were homogenized at 240 °C, for 5 min, in order to remove any thermal or solvent history,[18] after which the samples were cooled down to a given annealing temperature.

Unless otherwise stated, the DSC runs were performed employing a scan speed of 20 °C/min, using a Perkin-Elmer DSC-2. Temperature calibration of the calorimeter for all scan speeds used was performed with ICTA (the International Confederation for Thermal Analysis) certified reference materials. The heat of fusion of Indium was used for area calibrations.

Wide-Angle X-ray Scattering. The samples were analyzed with a Statton photographic X-ray camera using Ni-filtered Cu Kα radiation. The optical density of the films were measured by a Joyce-Loebl recording optical microdensitometer.

Results and Discussion

Main Characteristics of the DSC Traces. Completely amorphous homogeneous blends of 1:2 isotactic and syndiotactic PMMA (**i1** and **s1**) were annealed and afterward investigated by means of DSC, using a scan speed of 20 °C/min. To begin with, the main qualitative characteristics of the DSC traces in relation with the annealing conditions are given. In the following sections, we will present and discuss the exotherm and the endotherms in detail. For all cases, one glass transition of the blend (T_g) and a very small exothermic peak (T_x) at ≃130 °C was observed. The intensities of these transitions (i.e., the heats involved) decreased with increasing annealing time. In Figure 1 four characteristic DSC traces are given of samples differing in thermal history.

Without a thermal treatment, the samples show, besides the small exothermic transition (T_x), also a small endothermic transition with its maximum at $T_m^2 \simeq 166$ °C Figure 1a). Within experimental error, the absolute heats involved with these transitions are identical (0.3 J/g PMMA).

After annealing at low temperatures ($T_a < 125$ °C) for a relatively short time, three small strongly overlapping endotherms could be detected (Figure 1b) at temperatures T_m^1, T_m^2, and T_m^3. The heats involved, relative to each other, were a function of annealing time and temperature. In contrast to the first endotherm, the temperatures at which the second and third endotherm were detected appeared to be almost independent of thermal history, with

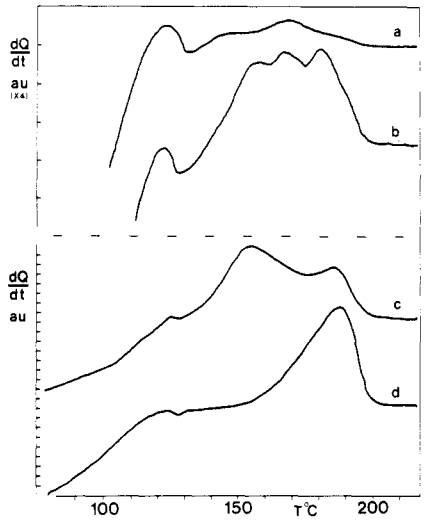

Figure 1. Representative DSC traces, employing 1:2 blends of **i1**/**s1**: (a) without a previous thermal treatment; (b) T_a = 110 °C, t_a = 2.5 h; (c) T_a = 110 °C, t_a = 16 h; (d) T_a = 140 °C, t_a = 2.5 h. The dQ/dT axis employed for curves (a) and (b) is extended 4 times as compared to the y-axis employed for (c) and (d).

values of ≃166 and 184 °C, respectively.

In the case of higher annealing temperatures (125 < T_a ≤ 135 °C) and/or longer annealing times only two endotherms were found (Figure 1c). The intensities of the endotherms with respect to each other appeared also to be a function of annealing time and temperature. Furthermore, in this case only the temperature at which the last endotherm is found (≃184 °C) was independent of thermal history.

Finally when the annealing temperature exceeds about 135 °C only one endotherm is found (Figure 1d). The temperature at which this transition is detected depends on thermal history.

The Exotherm. With respect to the small exotherm the following results were obtained:

On scanning a completely amorphous sample, apart from the exotherm at ≃130 °C an endotherm at ≃160 °C is also detected. Within experimental error the absolute heats involved with these transitions are identical.

The heat involved with the exothermic effect appears to be linearly dependent of the amount of material investigated.

When a sample is already annealed during longer times, the heat involved decreases.

It appears that the temperature T_x at which the effect is found coincides with the temperature at which the rate of complexation is at a maximum, as will be shown further on.

These observations point to the conclusion that during scanning, when the mobility of the chains is high enough, just beyond the glass transition, (additional) complexation occurs and an exothermic effect will be detected. This conclusion is supported by the fact that on using a 1:1 blend, resulting in a lowering of the glass transition temperature by about 15 °C, because of the lower glass transition temperature of i-PMMA, the exothermic effect is also shifted about 15 °C toward the lower temperature region. In addition to this, the endotherm broadens and also shifts toward lower temperatures. This endotherm identified as T_m^2 is now described as the temperature at which the complex formed during scanning decomplexes.[31] This explains also the independence of the location of this endotherm on thermal history. On using samples of high molar mass (**i2** and **s2**), it appears that the occurrence and intensity of the exothermic effect is virtually independent

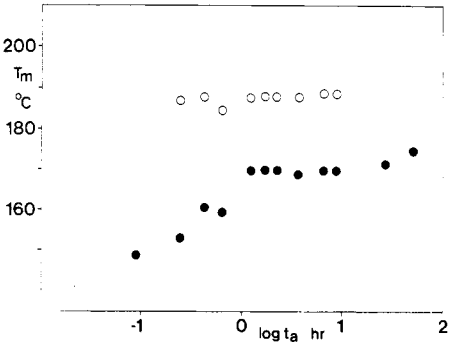

Figure 2. T_m^1 (●) and T_m^3 (○) as a function of annealing time at 125 °C in case of 1:2 blends of **i1**/**s1**. After longer annealing times T_m^3 could hardly be identified; these data are given as dotted circles.

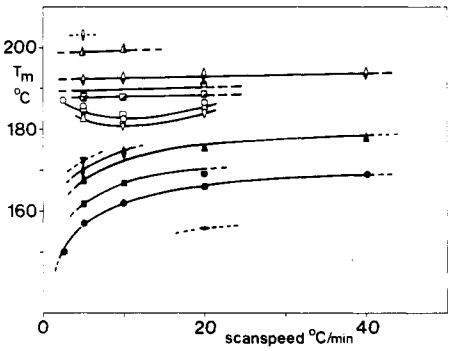

Figure 3. T_m^1 and T_m^3 as a function of scan speed, employing **i1**:**s1** 1:2 blends. t_a > 18 h, up to 20 days in the case of T_a = 165 °C. The filled symbols represent T_m^1 for T_a < 140 °C, whereas the open symbols represent T_m^3 next to T_m^1 in the same temperature region. (◒) 110 °C; (●, ○) 120 °C; (■, □) 125 °C; (▲, △) 130 °C; (◆, ◇) 132 °C; (▼, ▽) 135 °C. The half-filled symbols represent T_m^3 in case of annealing temperatures over 135 °C. (◪) 140 °C; (◓) 145 °C; (◇) 150 °C; (▲) 160 °C; (◒) 165 °C.

of the chain length of the components. This means that entanglements impose no limitations; segmental diffusion suffices, as can be expected in the case of complexation at conditions at which the critical sequence length for complexation is low (see also the section on the model).

The Endotherms. At lower annealing temperatures after relatively short annealing times, three small endotherms are detected (Figure 1b). As explained above, one of them, T_m^2 ≃ 166 °C, may be ascribed to the decomplexation of complex formed during scanning. After longer annealing times and higher annealing temperatures, the other endotherms will dominate the DSC trace and it is not possible to detect T_m^2 separately any more, as the heat involved is much lower than the heat involved with the other endotherms after longer annealing times (cf. Figure 1). Moreover, when higher annealing temperatures are employed, (125 < T_a < 135 °C) T_m^1 is shifted toward higher temperatures and coincides with T_m^2.

Now that the origin of T_m^2 is indicated, we will restrict ourselves to the remaining endotherms, T_m^1 and T_m^3. First we will show that the endotherms have different characteristics. Next we will show that, by use of polymers of relatively low molar mass like i1 and s1, the material giving rise to T_m^1 is (partly) transformed during scanning into material giving rise to T_m^3. In addition, we will show that the occurrence of the transformation depends on the molar masses employed. Finally we will show that the appearance of T_m^3 after annealing depends on the molar masses employed.

Some characteristic results on the remaining endotherms, employing 1:2 blends of i1 and s1, are given in

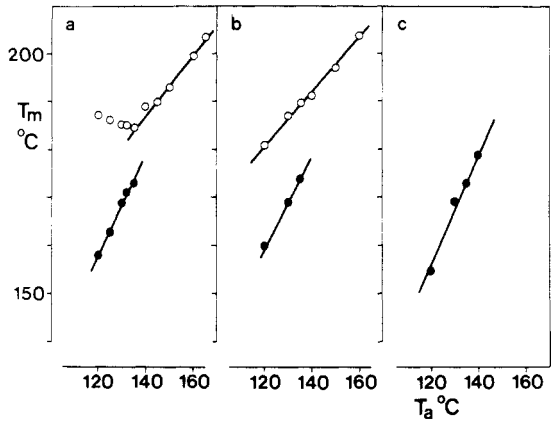

Figure 4. T_m^1 (●) and T_m^3 (○) as a function of annealing temperature for three different blends, differing in molar mass. t_a > 18 h, up to 15 days in the case of T_a = 160 °C. (a) 1:2 **i1/s1**, scan speed 5 °C/min; (b) 1:2 **i3/s3**, scan speed 10 °C/min; (c) 1:2 **i2/s2**, scan speed 5 °C/min.

Figures 2, 3, and 4a. In Figure 2, T_m^1 and T_m^3 are plotted as a function of the annealing time at T_a = 125 °C. Comparable figures were obtained for other annealing temperatures. Figure 3 gives T_m^1 and T_m^3 after different annealing temperatures as a function of scan speed. Finally Figure 4a represents a Hoffman–Weeks plot. With respect to the i1–s1 blend the following conclusions can be drawn: T_m^1 depends on annealing time and temperature in contrast to T_m^3 which only depends on thermal history in case of annealing temperatures over 140 °C (Figures 2 and 4a). T_m^1 displays a very strong superheating in contrast to T_m^3, as is shown in Figure 3. T_m^1 is found to be linearly dependent on annealing temperature with a slope of $\simeq 1$ (Figure 4a). In addition to this, we found the slope to be independent of scan speed. T_m^3 has virtually a constant value up to $T_a \simeq$ 135 °C on using a scan speed of 20 °C/min. On using a lower scanning rate, T_m^3 appears to decrease slightly as is shown in Figure 4a for the case of a scan speed of 5 °C/min. Above this temperature T_m^3 increases linearly ($T_m^3 = T_a$ at 280 °C). Careful examination of the various thermograms reveals that at lower annealing temperatures, T_m^1 is found after earlier annealing times and before T_m^3 can be detected. However, at higher annealing temperatures the order is reversed.

From these results, we may conclude that the endotherms have different characteristics. In addition to this, some of the results obtained are very similar to those met on investigating (partly) crystalline polymers in which recrystallization occurs. To investigate whether such a kind of reorganization is also important in this system, resulting in the transformation of material that gives rise to T_m^1 into material that gives rise to T_m^3, some additional experiments were performed.

First, the influence of the scan speed on the relative intensities of the endotherms was investigated. As a consequence of the strong overlap of the endotherms, especially at higher scan speeds because of the strong superheating performed by T_m^1, it is not possible to present quantitative results. Nevertheless, from the thermograms it was still possible to conclude that the relative intensity of T_m^3 (i.e., the heat involved) increases on decreasing the scan speed.

Next, some samples (T_a = 120 °C, t_a = 150 min) were partially scanned by using various scan speeds up to 160 °C, which is about halfway to the first endotherm. Immediately after this scan the samples were cooled down to 50 °C with a cooling rate of 60 °C/min and scanned again by using a scan speed of 20 °C/min. The results are presented in Table II. Unfortunately it was again not possible to separate the endotherms, therefore only a qualitative indication of the intensity of the endotherms with respect to each other is given.

Table II
Influence of a Partial Prescan up to 160 °C on ΔH_{1+3}, T_m^1, and T_m^3 and Their Relative Intensities[a]

scan speed, °C/min	ΔH_{1+3}, J/g	T_m^1, °C	T_m^3, °C	ΔH_1:ΔH_3
– (no prescan)	6.7	164	186	$\Delta H_1 > \Delta H_3$
10	6.4	175	186	$\Delta H_1 < \Delta H_3$
20	4.4	171	185	$\Delta H_1 \simeq \Delta H_3$
40	6.1	170	184	$\Delta H_1 \simeq \Delta H_3$
80	6.2	167	186	$\Delta H_1 > \Delta H_3$
160	6.4	166	186	$\Delta H_1 > \Delta H_3$

[a] As detected in the second (full) scan (20 °C/min), as a function of scan speed of the partial prescan. The polymer blend used is **i1:s1** 1:2. The samples were previously annealed at 120 °C for 150 min.

Table III
Influence of Annealing Time at 160 °C on ΔH_{1+3}, T_m^1, and T_m^3[a]

t_a, min	ΔH_{1+3}, J/g	T_m^1, °C	T_m^3, °C
0 (original sample)	6.7	164	186
0.5	4.1	170	185
1	5.3	(174)	184
5	6.3	—	186
60	6.4	—	189

[a] The polymer blend used is **i1:s1** 1:2. The samples were previously annealed at 120 °C for 150 min.

In addition, the samples with the same thermal history (T_a = 120 °C, t_a = 150 min) were annealed for short times at 160 °C. The results are given in Table III.

The results of these experiments confirm that material that gives rise to T_m^1 is transformed into material that gives rise to T_m^3 during the first scans. This is particularly apparent from the relative intensities of the endotherms and the increased values of T_m^1, especially after a prescan when lower scan speeds are used (Table II). Moreover, from the values of ΔH_{1+3} as a function of the scan speed (Table II) or annealing time (Table III) we can deduce that the material that gives rise to T_m^1 is not instantaneously transformed into the material that gives rise to T_m^3.

Further investigations, employing polymers of higher molar mass, showed that the molar mass is a very important parameter. In this case, with polymers of relatively low molar mass the mobility of the chains in the melt is high enough to make a reorganization process possible. On using a polymer pair of higher molar mass (**i3, s3**) a different Hoffman–Weeks plot is obtained (Figure 4b). In this case T_m^3 does not reach a constant value on lowering the annealing temperature but continues to decrease linearly with the same slope as obtained with **i1/s1**. Furthermore, in this system, reorganization during the scan was proved not to occur, employing the same experiments as described above.

From these results we have to conclude that both endotherms with different characteristics can be found independently and that T_m^3 is not necessarily formed during the scan. In the case of **i1/s1**, because of the low molar mass, it is possible that during the scan a transformation occurs resulting in an almost constant value of T_m^3 for low annealing temperatures. An important conclusion with respect to the transformation is that it requires the mobility of relatively long sequences.

A further increase of the molar mass results in a complete disappearance of T_m^3. On using **i2/s2**, in all cases only one endotherm is found, identified as T_m^1 from its

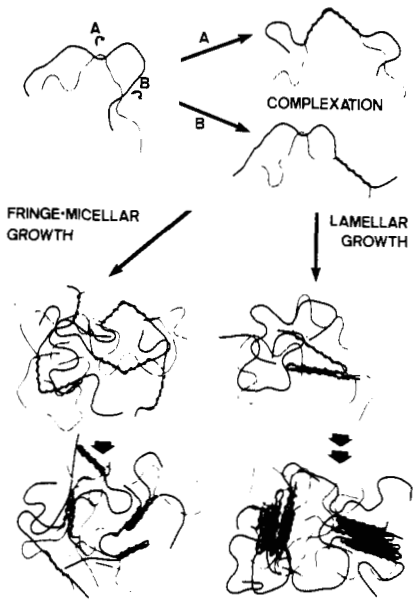

Figure 5. The mechanistic model, proposed for the overall complexation and crystallization process. First of all complex is formed via (a) "kink-nucleated complexation" or (b) chain end twisting (see text). Next, crystallites are formed by means of clustering of complexed sections (fringed-micellar growth) in the case of low annealing temperatures or lamellar growth in the case of high annealing temperatures.

behavior as a function of annealing temperature, as is shown in Figure 4c, which is identical, within experimental error, with the behaviour of T_m^1 for the case of **il/sl**. This endotherm also shows a considerable superheating. Another important observation is that after annealing at temperatures exceeding 145 °C, even the T_m^1 endotherm could not be detected anymore, unless annealing times of several days were employed.

From these results it appears that only the formation of the material that gives rise to T_m^3 requires the mobility of very long chain segments.

Mechanistic Model. Next, a mechanistic model to explain the results presented above will be presented and the observations will be discussed in relation with this model. In addition other experimental evidence will be presented and discussed. An important starting point not yet mentioned is that when material showing only T_m^1 is investigated by using WAXS, diffraction maxima are observed at the same angles as when material showing only T_m^3 is investigated. They only differ in intensity as will be shown further on. So both endotherms are related with a crystalline phase not differing in lattice structure. Another important point is that after heating up to 240 °C, which is just beyond T_m^3 complete decomplexation is attained.[18]

The model is represented schematically in Figure 5. The first step in the scheme comprises the complexation of chain sections which exceed the critical sequence length necessary for complexation. This critical length depends on the annealing temperature. A problem ignored up till now in the literature on this subject is how the double helices can be formed in bulk so quickly, while the movement of the chains is strongly hindered by entanglements. It is hard to imagine that the formation of double helices can only proceed by means of twisting the chains around each other, especially if one considers the fact that the molar masses of the polymers are no important limitation for the formation of complex. Moreover for the case of the **il:sl** 1:2 blend we have even found that complex is already formed at 100 °C which is only just above the glass transition temperature of the blend. From these arguments we expect that in bulk, simple twisting may occur only at the chain ends, as is indicated by complexation mode b in Figure 5. To explain the fact that chain length is no important limitation, we suggest that complexation can also start by means of forming a kink of s-PMMA, which subsequently wraps around an i-chain. Now, the complex nucleus can grow out by means of a simple rotation, as indicated by complexation mode a in Figure 5, resulting in a left-handed and a right-handed double helix next to each other. Even when other sections of the same chain are immobilized by entanglements or because of the fact that they already make part of another complexed section, complexation can still proceed by means of this "kink-nucleated complexation" mechanism.

After the formation of this complex nucleus, there are two possibilities for further growth. When the rate of complexation is much higher than the rate of crystallization, a scheme similar to "fringed-micellar" growth will be followed: all over the system, complexed sections are formed, which causes uncomplexed sections to become immobilized, and crystallization is only possible by means of clustering of the complexed sections.

Whenever complexation proceeds much slower, lamellar growth is possible. In this case the complex formed in neighboring segments will be stabilized directly by means of crystallization. The most important parameter that influences the rate of complexation as well as the rate of crystallization is the temperature. At low annealing temperatures the critical sequence length necessary for complexation is small, resulting in an enhanced rate of complexation. Lowering the annealing temperature also results in an increased melt viscosity while lamellar crystallization requires the mobility of much longer chain segments in comparison with complexation. So fringed-micellar growth can be expected to occur at lower annealing temperatures and consequently T_m^1 should be related to the melting of these crystallites while T_m^3 should be related to the melting of lamellar crystals. An indication that this is true is the observed superheating (Figure 3), which according to Wunderlich[27] is characteristic of the existence of crystallized tie molecules, arising in the case of fringed-micellar growth. The slope of 1 in the $T_m - T_a$ plot is also related to the existence of tie molecules.[28] Another important indication is that the molar mass of the polymers used is not important limitation for the formation of T_m^1, while T_m^3 is not found at all when polymers of high molar mass are used. This is understandable if one considers the fact that in the case of lamellar crystallization the chains must be completely free to move. In the case of long chains, different sections of the same chain are already immobilized as a consequence of complexation and the existence of entanglements, making reeling in, which is necessary for lamellar crystallization, impossible. Another important observation is that in the case of low annealing temperatures, T_m^1 is found somewhat earlier with respect to annealing time, before T_m^3 could be detected, while at higher annealing temperatures the order was reversed. This is also in line with the scheme presented above. At low temperatures, complexation proceeds faster than (lamellar) crystallization and consequently T_m^1 will be detected earlier. At higher annealing temperatures the predominant mechanism is lamellar growth until the system reaches immobilization and fringed-micellar growth becomes the only possible mode for further complexation and crystallization.

Now we have related the endotherms to different morphologies of the same crystal structure, it is necessary to

discuss the processes that give rise to these endotherms. We have referred at the beginning of this section to the fact that heating the samples beyond T_m^3 also results in decomplexation. According to Bosscher et al., the heat of stabilization of the complex itself is on the order of magnitude of 30 KJ/base mol of complex,[5] i.e., about 100 J/g of complex. During this study the maximum heat measured is on the order of magnitude of 20 J/g of polymer. Considering also the fact that up till now the largest dimensions of crystallites of stereocomplexes ever reported are only on the order of 10 nm[5,20] and consequently only consist of relatively few stereocomplex units, it is to be expected that the greater part of the heat involved with the endotherms should be ascribed to the heat of decomplexation. Thus we suggest that at both melting points for the major part the heat of decomplexation is detected.

With respect to the differences in melting point, it has to be remarked that a great difference in melting point between fringed-micellar and lamellar crystallites with the same lattice structure is not unusual. Differences on the order of 10–20 °C have been reported earlier.[29] The reason that T_m^3 has a higher value is that the complex is stabilized as a consequence of lamellar crystallization. Apart from the fact that in the case of fringed-micellar growth the crystallites cannot reach large dimensions for kinetic reasons, as the bulk is immobilized very quickly, this mechanism can also principally not result in larger crystallites because of the strong overcrowding of amorphous chain sections at the crystal–bulk interface. So these crystallites will have lateral dimensions of only a few strands of complexed material, not resulting in any important stabilization with respect to the noncrystallized complexed sections. In conclusion, according to our model, T_m^1 represents the decomplexation of complexed sections which are not lamellarly crystallized (i.e., uncrystallized and fringed-micellar crystallized complexes), while T_m^3 represents the decomplexation (and melting) of lamellarly crystallized complexes.

An important observation was that during the scan the material giving rise to T_m^1 seemed to be transformed into material giving rise to T_m^2 provided that the molar masses of the polymers used are low enough. This observation can now be explained in terms of the model presented above as that lamellar crystallites are able to grow at the expense of noncrystallized and fringed-micellar crystallized material. Before scanning, the greater part of the system is immobilized because of physical cross-links. On heating, when the temperature of decomplexation (T_m^1) is reached, depending on the length of the complexed sections, which is a function of thermal history, the system is not immobilized any more and the lamellar crystallites are now able to grow freely. The only condition is that the chain lengths of the polymers are not too high, otherwise reeling in is obstructed by entanglements. This is completely in line with the observed chain length dependence of the reorganization process.

In the next sections we will present and discuss other experimental evidence for the mechanism presented above.

Growth Kinetics. The total heat involved with both endotherms (ΔH_{1+3}) was measured as a function of annealing time and temperature. Some representative results are given in figure 6, top. It appeared that at low annealing temperatures no induction time can be detected, in contrast to annealing temperatures exceeding 135 °C, in which case an induction period is present. Another important finding is that at low annealing temperatures the total heat reaches a limiting value, earlier than in the case of higher annealing temperatures. Both observations are in line with

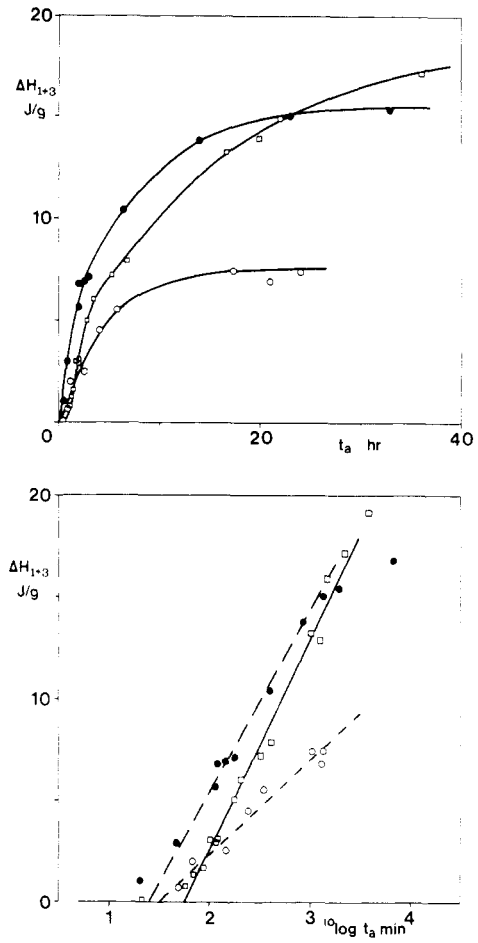

Figure 6. ΔH_{1+3} as a function of annealing time for the 1:2 **il/sl** blend for three different annealing temperatures: T_a = 110 (○), 120 (●), and 145 °C (□).

the proposed model. At low annealing temperatures the critical sequence length necessary for complexation is small and fringed-micellar growth will be the most important growth mode. In this case nucleation occurs almost instantaneously, so an induction period is not expected. Moreover, in this case a network is formed with complexed sections, partly organized into fringed-micellar crystallites, acting as physical cross-links, resulting in an immobilized system, which explains the fact that the limiting value is lower and is reached earlier than for the case of lamellar growth at higher annealing temperatures. In principle, in the case of lamellar growth the amorphous matrix is not influenced at all and a limiting value will only be reached when the system approaches the state of complete crystallinity. The observed induction period is inherent to the mechanism of lamellar growth, as a rather large nucleus has to be formed, in this special case a complex with the dimensions of the critical sequence length at the given temperature.

Next we have tried to estimate the maximum rate of growth as a function of the annealing temperature. Therefore ΔH_{1+3} was plotted as a function of log (t_a). Some representative examples are given in Figure 6, bottom. The result is a linear dependence for the major part of the data. From the slope and the intercept on the log (t_a) axis it is now possible to obtain a measure for the maximum growth rate at $\Delta H_{1+3} = 0$;

$$\left(\frac{\delta \Delta H_{1+3}}{\delta t_a}\right)_{\Delta H_{1+3}=0} = \frac{1}{t_a(\Delta H_{1+3}=0)\ \ln\ (10)}\left(\frac{\delta \Delta H_{1+3}}{\delta\ \log\ (t_a)}\right) \quad (1)$$

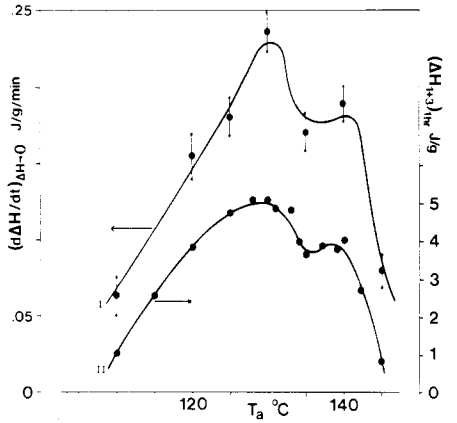

Figure 7. (I) Maximum growth rate of complexes and crystallites, in case of 1:2 **i1/s1** blends, as defined by eq 1 as a function of annealing temperature. (II) The total heat of decomplexation (and melting) ΔH_{1+3}, measured after annealing for 1 h at a given temperature T_a as a function of annealing temperature.

An important advantage of this method is that the experimental error is suppressed as the deviations in slope and intercept compensate each other.

From Figure 7 we can see that the maximum growth-rate curve shows two maxima. Although this result confirms the model, we have tried to verify these data. Therefore, the heat was measured after an annealing time of 1 h. Additional experiments were performed in order to obtain more data in the temperature region 125–145 °C. Finally, enthalpic data at 12 annealing temperatures in the mentioned region were collected. The results are also given in Figure 7. This procedure confirmed the existence of the two maxima.

As two mechanisms of growth are involved in the system under consideration, each with its own optimum temperature, this result was to be expected. At high annealing temperatures, first a complex nucleus of critical dimensions has to be formed, after which lamellar growth is possible. On lowering the temperature, the critical length decreases, but apart from this also the melt viscosity increases. So eventually, after an initial increase of the overall rate, as a consequence of the decreasing critical length, lamellar crystallization proceeds less fast because of the increasing viscosity, making reeling in of the chains more difficult. At still lower temperatures, the critical sequence length for complexation becomes so small that only segmental diffusion is sufficient to attain the critical dimensions. In this regime fringed-micellar crystallization becomes the predominant mode of growth, resulting in a second maximum in the growth-rate curve.

Influence of Melt Viscosity. From our model it appears that the mobility of the chains in the melt or the viscosity of the melt plays an important role. Especially lamellar growth is strongly hindered because it requires the mobility of much longer chain sequences. As i- and s-PMMA strongly differ in glass transition temperature, it is very easy to study the influence of melt viscosity by means of variation of the composition of the blend. Vorenkamp et al. have already found that because of the lower viscosity, the rate of complexation is higher in the case of an excess of i-PMMA, although the real composition of the complex at the level of monomeric units is still i/s = 1/2.[3] Various blends of **i4** and **s3**, which are of high molar mass, were annealed during one hour at 140 °C and were subsequently scanned. Reorganization during the scan appeared not to occur when these polymers are employed. The results are given in Figure 8. It appears that in the case of an excess of s-PMMA only T_m^1 is found. On

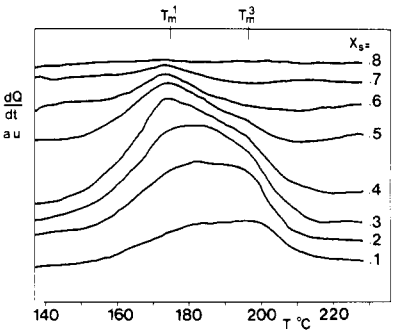

Figure 8. DSC traces of blends of **i4** and **s3** differing in compostion. The base mole fraction s-PMMA is given as X_s; T_a = 140 °C, t_a = 1 h.

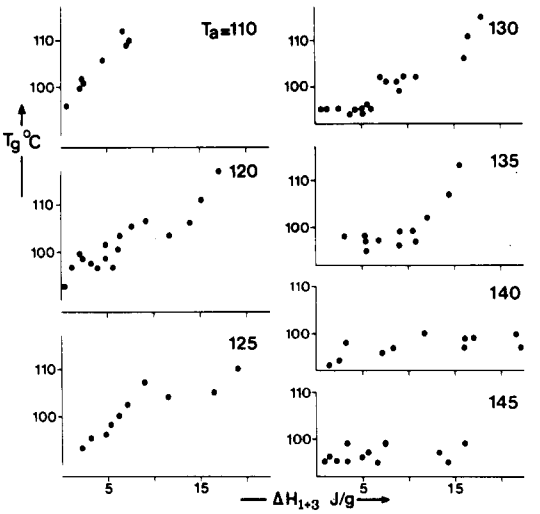

Figure 9. Glass transition temperature of 1:2 blends of **i1/s1** as a function of ΔH_{1+3}. The annealing temperatures employed are given in the figure.

increasing the relative amount of i-PMMA in the system, T_m^3 is also found next to T_m^1, and the relative intensity of T_m^3 increases as the amount of i-PMMA in the system increases, in line with expectations. Furthermore we can also clearly see the influence of the viscosity on the overall rate of complexation and crystallization as mentioned above. From this experiment we can see again the influence of the chain length. In case of blends, with polymers of low molar mass (**i1/s1**) only T_m^3 is found after annealing at 140 °C, while in this case, with polymers of higher molar mass, almost only T_m^1 is found at comparable compositions.

Glass Transition. If the stoichiometry of the complex is the same as the composition of the blend (1/2 i-/s-PMMA), the study the glass transition temperature of the bulk as a function of the thermal history of the sample without considering a change in composition of the bulk is permitted. Furthermore, the complex itself does not have a glass transition.

In order to make it possible to compare the results after different annealing temperatures and times, the temperature of the beginning of the glass transition is plotted in Figure 9 as a function of the total heat involved with the endotherms, ΔH_{1+3}, which is a measure of the degree of complexation (and crystallization).

At lower annealing temperatures (T_a < 130 °C) the glass transition temperature increases monotonously with the enthalpic value of the system. Between 130 and 140 °C, a sort of period of induction is observed after which the glass temperature starts to rise. At still higher tempera-

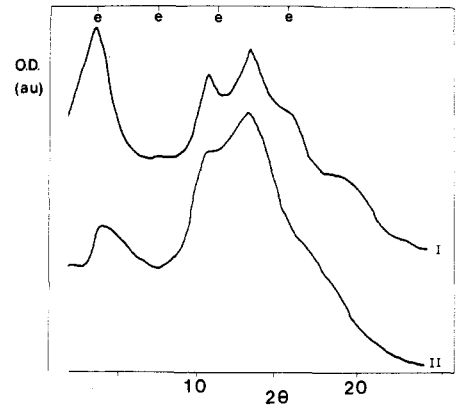

Figure 10. Optical density of two röntgen films as a function of the angle of diffraction. The samples investigated were annealed at 160 °C (I) and 120 °C (II) for 20 days and 32 h, respectively, resulting in comparable values of ΔH_{1+3} (16.2 and 15.1 J/g, respectively).

tures the glass temperature is not influenced by the annealing process. With respect to the ΔC_p jump, it is found that it decreases when the amount of (crystalline) complex increases. Unfortunately it appeared not to be possible to measure quantitatively ΔC_p, as the beginning of the first endotherm is found very close to the end of the glass transition, especially after low annealing temperatures. Nevertheless it appeared that after prolonged annealing times, especially after a thermal treatment at low temperatures, hardly a ΔC_p jump could be detected, although the amount of complexed material, as derived from the heats involved with the endotherms, was at maximum half the amount found after complexation in dilute DMF or acetone solutions.[30]

These results are also consistent with the proposed model. At low annealing temperatures only complexes and fringed-micellar crystallites of complexes are formed. The overall system will be increasingly immobilized and also the mobility of the noncomplexed chain sections will be strongly hindered. In this case a strong influence on the glass transition temperature can be expected and is also found. On the other hand, in the case of lamellar growth, in principle the amorphous matrix is not influenced, which explains the constancy of the glass transition temperature after annealing at higher temperatures. In the case of moderate annealing temperatures ($130 < T_a < 140$ °C), the growth mode appeared to have primarily a lamellar character until, because of the increasing immobility of the system, only fringed-micellar growth is still possible. In this case the term "secondary crystallization", used by Vorenkamp et al. in relation with the first endotherm,[3] is correct. Nevertheless, as is shown for very long chains, in which case only T_m^1 is found, this mode of crystallization is not principally of secondary nature.

WAXS. In principle it is possible that the different endotherms, T_m^1 and T_m^3, arise from the melting of different crystallites with a different lattice structure or that one endotherm is correlated with the decomplexation and the other with the melting of crystalline complex. Neither of these possibilities appears to be true because the same diffraction pattern is always observed, as was also found by Vorenkamp et al.[3] Only differences in intensity of diffraction maxima could be detected. Nevertheless, careful examination of these differences in relation to the results of Bosscher et al. on the fiber diffraction patterns of stereocomplexes[5] appeared to be very useful. In Figure 10 the WAXS patterns of samples annealed at 120 and 160 °C, containing the same amount of (crystalline) complex as found by means of DSC (ΔH_{1+3} of both samples are comparable) are given. In the case of fiber diffraction, four reflections are found on the equator and consequently correspond to ordering perpendicular to the helix axis. The locations of these reflections are indicated in Figure 10. It is clear that in the case of the 160 °C sample these "equatorial" reflections are relatively much stronger than in the case of the sample annealed at 120 °C. This result is again in line with the model. At 120 °C the predominant mechanism is fringed-micellar growth, resulting in only small bundles of helices. In this case the ordering parallel to the helix axis will dominate the diffraction pattern. At 160 °C only lamellar crystallization is possible. In this case ordering perpendicular to the helix axis is also important and the corresponding reflections will be found stronger.

Concluding Remarks

In this paper the results of a study of the complexation between i- and s-PMMA in bulk are presented. To explain the observed phenomena a mechanistic model is proposed in which crystallization of stereocomplexes plays a dominant role. According to this model, in principle two different mechanisms can be followed, viz., fringed-micellar versus lamellar crystallization. The critical sequence length for complexation and the mobility of the chains, and consequently the annealing temperature and molar mass of the polymers, are the most important parameters. By introducing the so-called "kink-nucleated" mechanism for complexation, the model also accounts for the fact that the formation of complexed sections consisting of double-helices proceeds very fast in bulk and is not limited by chain lengths.

Although we have tried to prove the existence of lamellar crystallites directly by means of optical microscopy, these attempts have not been successful yet, despite the application of high annealing temperatures, up to 180 °C, for months. Apparently, the crystallites are too small. Considering the fact that a crystal consisting of two different polymers has to be formed, while those polymers are never perfectly tactic, we can understand that, because of crystal defects resulting from the imperfectness of the polymers with respect to tacticity as well as the increased importance of defects related with the chain ends of the polymers as compared to "normal" polymer crystals, it is very difficult to obtain crystals of large dimensions from the bulk. Although we have presented various data which can be taken as indirect evidence supporting the model, we were unfortunately not able to obtain direct evidence. Nevertheless we have shown that with this model it is possible to explain all the phenomena observed in terms of it.

From these results it is to be expected that in the case of complexation in (dilute) solution, crystallization is also an important factor, especially if one considers the association phenomena, reported earlier, leading to very compact particles of about 10–30 nm.[11,13-17] As a matter of fact, multiple endotherms shown by complexed material obtained from dilute solution have already been reported.[6,21,22] In a following paper the results of an investigation on the role of crystallization in the stereocomplexation process in dilute solution will be presented.[30] It appears that in principle the same mechanistic scheme can account for the observed phenomena.

Registry No. i-PMMA, 25188-98-1; s-PMMA, 25188-97-0.

References and Notes

(1) Fox, T. G.; Garrett, B. S.; Goode, W. E.; Gratch, S.; Rincaid, J. F.; Spell, A.; Stroupe, J. D. *J. Am. Chem. Soc.* **1958**, *80*, 1768.
(2) Liquori, A. M.; Anzuino, G.; Coiro, V. M.; D'Alagni, M.; de Santis, P.; Savino, M. *Nature (London)* **1965**, *206*, 358.
(3) Vorenkamp, E. J.; Bosscher, F.; Challa, G. *Polymer* **1979**, *20*, 59.

(4) Bosscher, F.; Keekstra, D. W.; Challa, G. *Polymer* **1981**, *22*, 124.
(5) Bosscher, F.; ten Brinke, G.; Challa, G. *Macromolecules* **1982**, *15*, 1442.
(6) Challa, G.; de Boer, A.; Tan, Y. Y. *Int. J. Polym. Mater.* **1976**, *4*, 239.
(7) Katime, I. A.; Quintana, J. R. *Makromol. Chem.* **1986**, *187*, 1441.
(8) Mekenitskaya, L. I.; Amerik, Yu. B.; Golova, L. K. *Vysokomol. Soyedin., Ser. A* **1979**, *A21*, 1334; *Polym. Sci. USSR (Engl. Transl.)* **1980**, *21*, 1463.
(9) Vorenkamp, E. J.; Challa, G., *Polymer* **1981**, *22*, 1705.
(10) Belnikevitch, N. G.; Mrkvičková, L.; Quadrat, O. *Polymer* **1983**, *24*, 713.
(11) Schomaker, E.; ten Brinke, G.; Challa, G. *Macromolecules* **1985**, *18*, 1930.
(12) Schomaker, E.; Vorenkamp, E. J.; Challa, G. *Polymer* **1986**, *27*, 256.
(13) Spěváček, J.; Schneider, B. *Makromol. Chem.* **1974**, *175*, 2939.
(14) Khodakov, Yu. S.; Berlin, Al. Al.; Kalyayev, I. I.; Minachev, Kh. M. *Zh. Teor. Eksp. Khim.* **1969**, *5*, 631.
(15) Kabanov, V. A.; Papisov, I. M. *Polym. Sci. USSR (Engl. Transl.)* **1979**, *21*, 261.
(16) ten Brinke, G.; Schomaker, E.; Challa, G. *Macromolecules* **1985**, *18*, 1925.
(17) Schomaker, E.; Challa, G. *Macromolecules* **1986**, *19*, 2841.
(18) Feitsma, E. L.; de Boer, A.; Challa, G. *Polymer* **1975**, *16*, 515.
(19) Liu, H. Z.; Liu, K. I. *Macromolecules* **1968**, *1*, 157.
(20) Könnecke, K.; Rehage, G. *Colloid Polym. Sci.* **1981**, *259*, 1062.
(21) de Boer, A.; Challa, G. *Polymer* **1976**, *17*, 633.
(22) Katime, I.; Quintana, J. R.; Veguilas, J. *Thermochim. Acta* **1983**, *67*, 81; *Polymer* **1983**, *24*, 903.
(23) Goode, W. E.; Owens, F. H.; Feldmann, R. P.; Snijder, W. H.; Moore, J. H. *J. Polym. Sci.* **1960**, *46*, 317.
(24) Abe, H.; Imai, K.; Matsumoto, M. *J. Polym. Sci., Part C* **1968**, *23*, 469.
(25) Lando, J. B.; Semen, J.; Farmer, B. *Macromolecules* **1970**, *3*, 524.
(26) de Boer, Th.; Backer, H. J. *Recl. Trav. Chim. Pays-Bas* **1954**, *73*, 229.
(27) Wunderlich, B. *Macromolecular Physics III*; Academic: New York, 1980; pp 223–224.
(28) Lemstra, P. J.; Kooistra, T.; Challa, G. *J. Polym. Sci., Part A-2* **1972**, *10*, 823.
(29) Berghmans, H.; Govaerts, F., Overbergh, N. *J. Polym. Sci., Polym. Phys. Ed.* **1979**, *10*, 823.
(30) Schomaker, E.; Hoppen, H.; Challa, G. *Macromolecules*, following paper in this issue.
(31) According to the mechanistic model, described in this paper, T_m^1 represents the decomplexation of complexed sections, partly clustered into fringed-micellar crystallites. As it is not to be expected, because of kinetic reasons, that during scanning complexation and clustering of the complexes formed take place, T_m^2 is assigned to only the decomplexation of the complexed sections, formed during scanning.
(32) Mahabadi, H. Kh. *J. Appl. Polym. Sci.* **1985**, *30*, 1535.
(33) Jenkins, R.; Porter, R. S. *J. Polym. Sci., Polym. Lett. Ed.* **1980**, *18*, 743.
(34) Rudin, A.; Holgy, H. L. W. *J. Polym. Sci., Polym. Chem. Ed.* **1972**, *10*, 217.

Complexation of Stereoregular Poly(methyl methacrylates). 12. Complexation Process in Dilute Solution

Elwin Schomaker, Henk Hoppen, and Ger Challa*

Laboratory of Polymer Chemistry, State University of Groningen, Nijenborgh 16, 9747 AG Groningen, The Netherlands. *Received July 22, 1987; Revised Manuscript Received November 13, 1987*

ABSTRACT: The process of stereocomplexation between isotactic and syndiotactic PMMA in dilute solution was studied by means of differential scanning calorimetry of isolated complexed material, solution viscometry, and isothermal mixing calorimetry. The results were combined with results of investigations previously published. It appeared that essentially the same mechanism as proposed for the complexation process in bulk can account for the observed phenomena, including the previously reported association and aggregation stages following complexation. Two main processes are distinguished: complexation and subsequent crystallization of complexed chain sections, leading to the formation of complex particles. With respect to crystallization, two modes are suggested: fringed-micellar and lamellar growth, depending on the so-called critical sequence length under the conditions employed and the mobility of the chain sections. These parameters appear to be influenced by various variables such as solvent quality, temperature, mixing ratio, and tacticity.

Introduction

Stereocomplexation of isotactic and syndiotactic poly(methyl methacrylate) (i- and s-PMMA) is possible in (dilute) solution as well as in bulk. In a companion paper the results were given of an investigation on the overall process in bulk and a mechanistic model which accounts for the observed phenomena was presented.[1]

With respect to dilute solution one can distinguish three kinds of solvents: strongly complexing, weakly complexing, and noncomplexing, respectively designated as solvent type A, B, and C.[2,3] In addition to this it was found that the "complexing ability" of a solvent can be changed from type A to eventually type C by raising the temperature.[2,4] Although various investigators have tried to correlate the complexing ability of solvents to solvent characteristics, a satisfactory correlation was not yet achieved.[2,3,5-7] In the case of strongly complexing solvents, complex particles are formed of about 10–30 nm,[4,8-11], consisting of a compact nucleus surrounded by a shell of noncomplexed chains.[4,9] In the case of an excess of one of the components this shell consists of the component in excess, leading to steric stabilization of the complex particles.[4,9] Schomaker et al. have given a phenomenological description of the process.[4] They showed that in case of solvents of type A, three stages can be distinguished: (i) complexation: (ii) association of complexed chain sections resulting in the formation of compact "complex particles"; (iii) aggregation of complex particles, eventually followed by flocculation.

As complexed material obtained from dilute solution also shows crystallinity,[5,12-16] and as also is found that on employing a strongly complexing solvent two melting points are found,[14,15] we investigated whether the same mechanism as proposed for complexation in bulk is followed in dilute solution.

In this paper the results of the present investigation on the complexation process in dilute solution are discussed, in combination with the results of previously published investigations, in terms of the mechanism proposed for the complexation in bulk.[1] First we show that the observed melting endotherms, shown by material obtained from

0024-9297/88/2221-2203$01.50/0